Experimental Investigation of the Periodicity in a Sector of an Annular Turbine Cascade

Wiers S.-H.
Phone: +46 8 790 61 40
E-mail: sven@egi.kth.se

Fransson, T. H.
Phone: +46 8 790 7467
E-mail: fransson@egi.kth.se

Fax +46 8 204161
Chair of Heat and Power Technology
Royal Institute of Technology
Brinellvägen. 60
100 44 Stockholm, Sweden

ABSTRACT

Due to the necessity of more detailed three-dimensional data on the behavior of film cooled blades an annular sector cascade turbine test facility has been taken into service. The annular sector cascade facility is a relative cost efficient solution compared to a full annular facility to investigate three-dimensional effects on a non cooled and cooled turbine blade.

The aerodynamic investigations on the annular sector cascade facility are part of a broad perspective where experimental data from a hot annular sector cascade facility and the cold annular sector facility are used to verify, calibrate and understand the physics for both internal and external calculation methods for flow and heat transfer prediction.

The objective of the present study is the design and validation of a cold flow annular sector cascade facility, which meets the flow conditions in a modern turbine as close as possible, with emphasis on achieving periodic flow conditions.

Intensive experimental work with six different test section set ups have been carried out to optimize the flow conditions up- and downstream of the cascade. The influence of tailboards as well as the use of two different kind of diffusers, one with an opening angle of 12^o and the other a step diffuser, has been investigated. Satisfactory results could be achieved with respect to homogeneous inlet flow conditions and the periodicity of the flow filed in a set up without tailboards mounted and a step diffuser. In this case the exit flow develops as a free jet and the flow angle adjusts itself to the downstream back pressure.

NOMENCLATURE

c	Turbine blade mechanical chord
c_{ax}	Axial chord
t	Pitch
ΔM	Mean deviation
M_1	Inlet Mach number
M_2	Outlet Mach number
n	Number of flow passages
p	Pressure
p_1/p_2	Pressure ratio
r	Range
Re	Reynolds number
T_o	Total temperature
T_u	Inlet turbulence level

Greek

α	Flow angle
γ	Stagger angle
Π	Pressure ratio
Φ	Circumferential coordinate
ρ	$[kg/m_3]$ Density

Subscripts

ax	Axial
iso	Isentropic
LE	Leading edge
inlet	Inlet
out	Outlet
stat	Static
atm	Atmosphere
∞	Mainstream

INTRODUCTION

The increase of efficiency of gas turbines is directly related to a higher pressure ratio. This means also higher inlet temperature in the turbine. Common turbine blade materials are not able to withstand the high thermal demands without cooling. The result of the ongoing development in the last 40 years is a highly complicated cooling mechanism, usually a combination of impingement-, convection-, and film cooling. Due to this an increase of the turbine inlet temperature of 800 K was possible. Today a maximum inlet temperature of 1800 K is realistic. But the potential of improvements have not reached a limit. New complicated cooling mechanisms combined with new materials, as well as coating with ceramics will ensure a steady ongoing increase of the turbine inlet temperature. Film cooling is a very efficient solution to protect the blade surface. The compressed air by passes the combustion chamber and is then blown through slots or angled holes on the surface of the turbine blades. A cooling film is generated which guards the blades against the hot gases. At the same time an interaction of the injected cooling air with the

main flow takes place. This interaction has unwanted effects on the local cooling efficiency and on the aerodynamic properties of the cascade.
The secondary flow that occurs in each cascade has a large influence on the loss behavior of the cascade. This secondary flow causes a collection of loss producing boundary layer flow in the hub and tip region. The interaction of film cooling with secondary flow causes a very complex flow pattern. The highest priority for the efficiency of a gas turbine cycle is a minimum need of cooling air with an optimum of cooling and at the same time as low as possible aerodynamic losses. The requirement for that is a detailed knowledge of the cooling jet exit flow and its mixing behavior as well as the phenomena of the secondary flow and the parameters that influence this phenomenon. To be able to gain a full understanding of the aerodynamic behavior of a turbine cascade and the heat transfer process one step in the direction of achieving this, is to test the same engine components in a cold flow test facility which give the possibility of detailed aerodynamic investigations and tests at "near-engine conditions" which give a better understanding of the heat transfer process [Rådeklint, 1998, 1999]. This has been realized by setting up a cold flow and a hot flow annular sector cascade, which are identical.
Two kinds of cold flow cascade test facilities are well know in the open literature: The linear cascade and the full annular cascade both of them having advantages and disadvantages. Descriptions of cold flow linear cascade can be found for example in Yamamoto [1987], Curties et al. [1996] and also in Hoffs [1996]. Full annular cascade facilities are described in Kobayashi [1988], Wegener et al. [1989] and Bölcs [1983].
Due to the necessity of more detailed 3-D aerodynamic data on the behavior of film cooled blades it was decided to build up an annular sector turbine cascade test facility at KTH [Wiers, 1998, 1999].

EXPERIMENTAL APPARATUS

A schematic view of the layout of the annular sector cascade facility is shown in Fig. 1. The test facility has been designed with the objective to investigate the steady state 3D flow conditions on a modern full-scale nozzle guide vane with and with out film cooling.
The test facility consists of the following main parts:

- Compressor
- Air cooler
- Bypass valve
- Settling chamber which contains a honeycomb and mesh screens
- Exchangeable turbulence grid
- Inlet traversing ring
- Test section
- Outlet diffuser with exchangeable tailboards

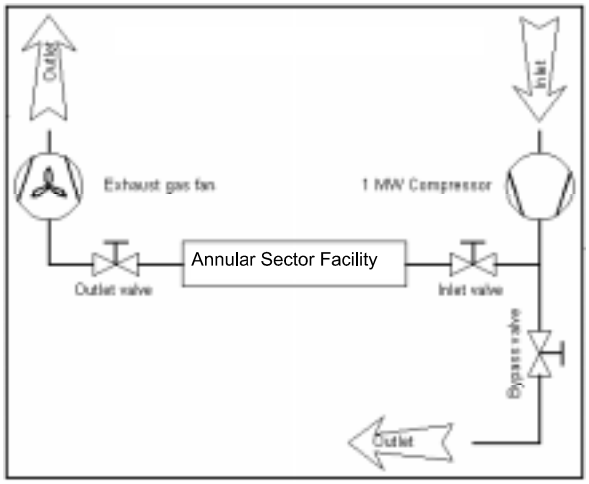

Fig. 1 *Schematic of annular sector facility*

The air to the test facility is supplied from an electric motor-driven screw compressor that can deliver a continuous flow up to 4,7 kg/s at 4 bar.
The air exhaust temperature is 180^{o}C, this temperature can then be varied by a cooling system between 180^{o}C and 30^{o}C.
The mass flow from the compressor is controllable by the inlet valve and the bypass valve which are located in front of the test facility. The total pressure is adjustable with an outlet valve which is connected to the exhaust gas fan, due to this an independent variation of Mach and Reynolds number is possible.

TEST SECTION.

The test section inlet is designed like the outlet of the combustion chamber of a full-scale modern gas turbine. Due to this shape real engine flow conditions have been reproduced Fig. 2.

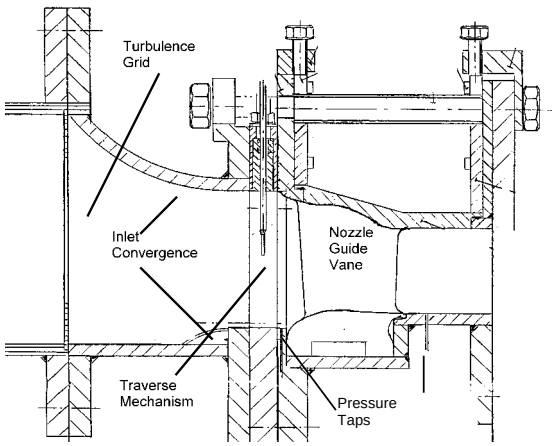

Fig. 2 *Test section*

Different turbulence grids can be placed 160 mm upstream of the nozzle guide vanes. A traversing mechanism to traverse pressure and hot wire probes in radial and circumferential direction is located between the inlet convergence and the nozzle guide vanes. The test section geometry limits the circumferential traversing length to a sector of 19.7^{o}.

Experimental conditions

The investigated cascade has an inlet angle of 90° and an outlet blade angle of 15.1°. The blade chord at mid-span is 110.4 mm which gives an aspect ratio at the inlet of H_{inlet}/c= 0.77 and an aspect ratio at the outlet of H_{out}/c = 0.53.

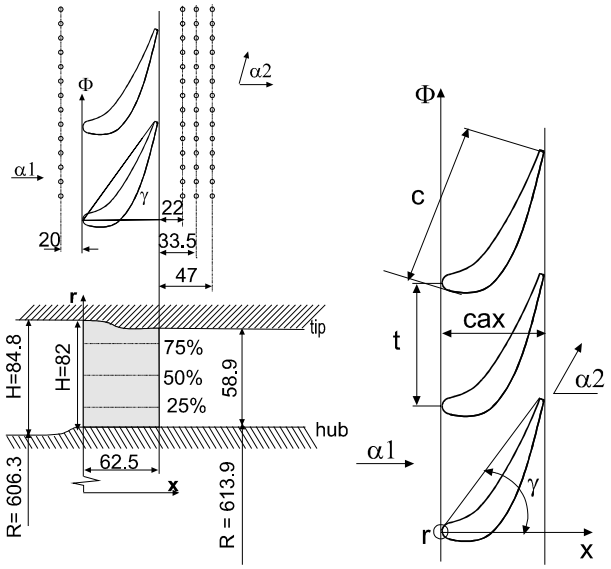

Fig. 3 *Cascade geometry*

An unrolled surface of the annular cascade at mid-channel is presented in Fig. 3. The blade geometry and nominal conditions at midspan are given in Table 1. The coordinate system is defined as following: x in axial (flow) direction from the leading edge at hub, r in radial (outward) direction from the central axis and Φ in circumferential (anti-clockwise) direction from the leading edge of blade number "0". The coordinate system as well as angular definitions can be found in Fig. 3.

number of blades	6
t	7.2^o
$c_{midspan}$	110.4 mm
$c_{axmidspan}$	65.7 mm
H_{inlet}/c	0.77
H_{outlet}/c	0.53
γ	50.4^o
$M_{1midspan}$	0.1
α_1	90^o
$M_{2ismidspan}$	0.9
$\alpha_{2midspan}$	15.1^o
p_{tot}	2.1 bar
p_2	1.3 bar
Π	1.64
T_{tot}	303 K
Re_c	$5.7*10^5$

Table 1 *Design test conditions*

The measuring equipment

A parallel-processing pressure acquisition system, with a total amount of 208 channel is used to measure the static pressure up- and downstream of the blades, steady state pressure on the blade surfaces of blade +1, 0 and -1. It is also used to measure the total pressure p_0 in the settling chamber.

The system 8400 is a highly modular data acquisition system, supporting unique electronic pressure scanners and pressure standards. The host for this system can be any computer that supports the GPIB/IEEE-488 interface. The main chassis is the System Processor (SP), which contains a central 32-bit microprocessor, host interface (GPIB), and high speed input unit interface. The System 8400's data acquisition and pressure generation functionality is provided by discrete input units. Multiple types of input units are available to provide specific functions. Every Unit also has a 64180 8-bit CPU with firmware, logic control, and 256K bytes of local memory. The Scanner Digitiser Unit (SDU) performs efficient analog-to-digital conversion of the analog signal from multiple local or remote pressure scanners. Data from each scanner pressure port are received via the scanner interface and converted to a 16-bit raw data words. The Pressure Calibration Unit (PCU) is a digitally controlled pneumatic calibration source and/or pressure generator. The Pressure Standard Unit is a PCU with a high accuracy pressure standard transducer to read only reference pressures.

Rapid connectors with 52 channels each are used to multiplex the huge amount of pressure taps in the annular sector cascade with the 104 channels of ±100 kPa pressure scanners. Those have an accuracy of ±50 Pa. The used 35 kPa scanners have an accuracy of ±17.5 Pa.

TYPICAL INSTRUMENTATION OF THE TEST SECTION

The total temperature in the settling chamber is measured by a K-type thermocouple with a sensibility of 40 μV/ °C and an accuracy of ±0.4 °C for the temperature range 10-40 °C. The thermocouple is connected via a PC-logger to a standard PC where the data is stored on the hard disk.

The total pressure is measured at three different locations, up and downstream of the settling chamber and downstream of the turbulence grid.

The reason is the determination of the pressure drop over the honey comb and the mesh screens in the settling chamber as well as the pressure drop over the different turbulence grids. The total pressure probe which is used has a maximum angle of attack of ± 24 ° where the measured total pressure deviates less than 0.3% of the true total pressure.

The atmospheric conditions P_{atm} and T_{atm} are synchronously measured with the static and total pressure measured with the PSI-system[1] by the use of a Solatron[2] barometer which is connected to a PC. The accuracy of the barometer is ±10 Pa.

The inlet pressure distribution is measured by traversing a 3 hole pressure probe in a sector of

[1] Pressure System Incorporation
[2] Company name

19.7^0 between NGV "-1" and "+1", 54% upstream of the NGV, in steps of 5 mm in radial direction and 2^o in circumferential direction. This leads altogether to 209 measuring points.
35 pressure taps equal distributed at the hub -33% upstream of c_{ax} are used to measure the inlet Mach number distribution across all six flow passages (Fig. 4).

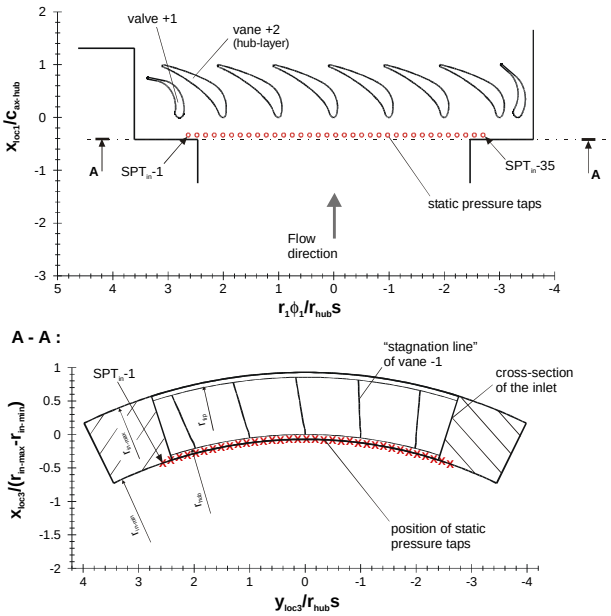

Fig. 4 *Pressure taps upstream at the hub*

Vane Surface Velocity Distribution: In order to obtain detailed information about the 3-D influence on the velocity distribution across the blade surface vane number "0" is equipped with 58 pressure taps distributed at 75, 50 and 25 percent of span$_{LE}$[3] on the suction and pressure side Vane "-1" is equipped with 23 pressure taps equally distributed at 25 percent of span$_{LE}$[3] on the pressure side. Vane "+1" is equipped with 23 pressure taps equally distributed at 75 percent of span$_{LE}$[3] on the suction side. Due to this information about the periodicity of the flow field through flow passage "-1" and "+1" can be gained.
Tip Endwall Velocity Distribution: 126 pressure taps in a window which covers the whole flow passages "-1"and "+1" are used to monitor the Mach number distribution across the flow passages**.** The exact location of the pressure taps is shown in Fig. 5.

[3] Due to the three dimensional shape of the NGV the span changes with the chord

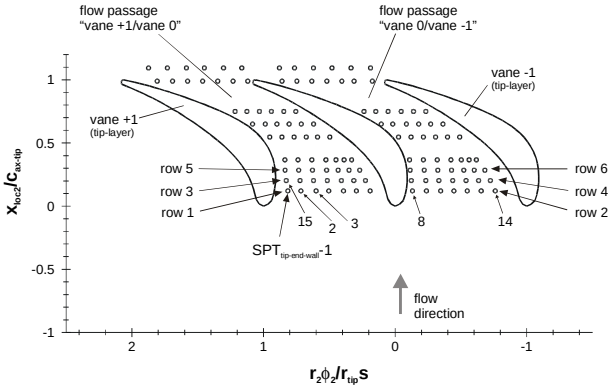

Fig. 5 *126 pressure taps distributed across flow passage "-1" and "+1"*

Outlet Flow Conditions The outlet velocity and pressure distribution is obtained by traversing five hole pressure probes [Wiers 2000] over a sector of 17^0.
The static pressure distribution downstream at the hub is measured with 60 pressure taps equally distributed at 135.2%, 153.6% and 175.2 % of axial chord (Fig. 6)

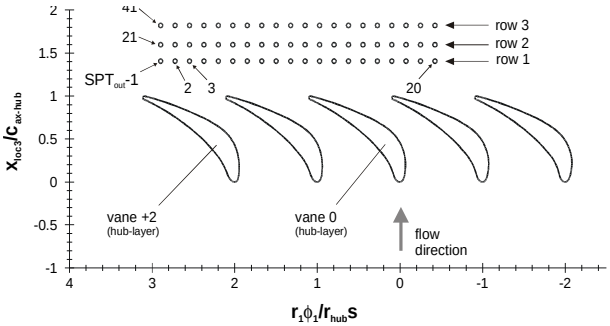

Fig. 6 *Static pressure taps at the outlet of the test section*

RESULTS

Periodic flow conditions is a key for accurate measurements in cascade facilities. In linear cascade facilities periodic flow conditions have been realized by using tailboards and slotted side walls. There is little experience about periodic flow conditions in annular sector cascades and how to achieve this published in the open literature. Due to this, five different test section setups with and without tailboards and also different outlet diffuser configurations have been investigated. The five different setups are described below. Due to the fact of a circumferential variation in location of the corresponding pressure taps in flow passage -1 and +1 trend lines have been used to make the isentropic Mach number distributions at the several axial position in both flow passages comparable. The graphs show a comparison of the actual isentropic Mach number distribution, the mean deviation from $\Delta M = 0$, the standard deviation and the range is also given for each axial M_{iso} distribution.

<u>Setup with tailboards and diffuser mounted (case 1)</u>
In linear turbine cascade facilities tailboards are used to generate a periodic down stream flow field.

The same principle has been applied to the annular sector cascade facility, due to the annular shape of the upper and lower end walls it was not possible to use moveable tailboards. The tailboard mounted on vane -3 has an opening angle of $+4^0$ and the tailboard mounted on vane +2 an opening angle of -3^0. A diffuser with an opening angle of 12^0, to guide the flow smoothly into the outlet, has been mounted at the outlet 190% downstream of axial chord.

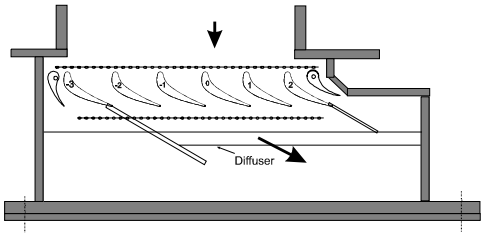

Fig. 7 *Setup with tailboards and diffuser mounted*

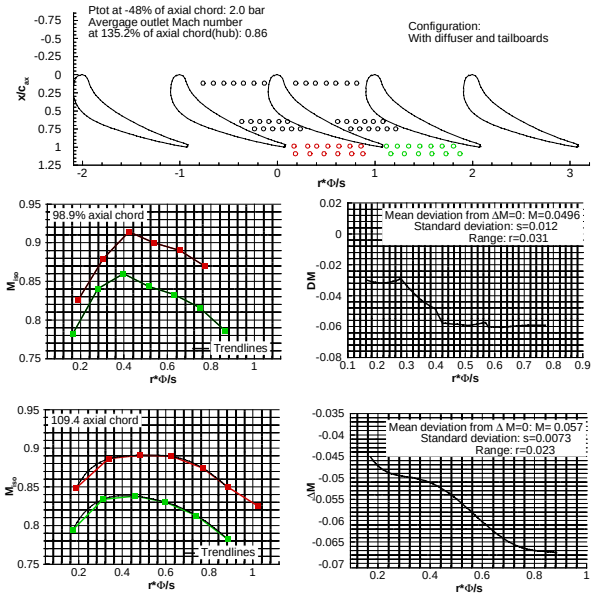

Fig. 8 *Tip M_{iso} distribution at 98.9% and 109.4% of axial chord (case 1)*

The measured M_{iso} distribution at 98.9% and 109.4% of axial chord at the tip is illustrated in Fig. 8. The periodicity of the flow field decreases dramatically towards the outlet. This fact leads to the conclusion that either the diffuser or the tailboards have an influence on the outlet flow conditions. The mean deviation ΔM, standard deviation s and the range r for the these three axial locations are given in Table 2.

	98.9%	***109.4%***
case 1		
ΔM	0.049	0.057
s	0.012	0.007
r	0.031	0.023

Table 2 *ΔM, s, r in case 1 at 98.9% and 109.4% of c_{ax}*

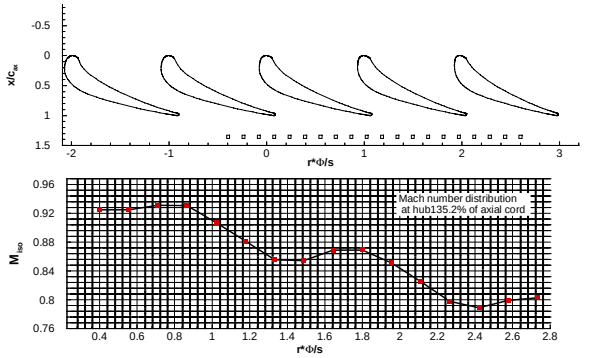

Fig. 9 *Hub M_{iso} distribution at 135.2% of axial chord (case 1)*

The outlet M_{iso} distribution measured at 135% of axial chord at the hub shown in Fig. 9 indicates the same decreased periodic outlet flow conditions as at the tip.

<u>Setup with tailboards and without diffuser (case 2)</u>
The results of the outlet M_{iso} distribution at the tip (Fig. 8) and hub (Fig. 9) obtained in case 1 show a non periodic flow field. Due to this fact in case 2 the outlet diffuser has been changed from a continuos cylindrical diffuser to a step diffuser which gives a certain defined separation point of the outlet flow. The philosophy of the tailboards has been kept to adjust the outlet flow angle and to guide the flow in circumferential direction (Fig. 10).

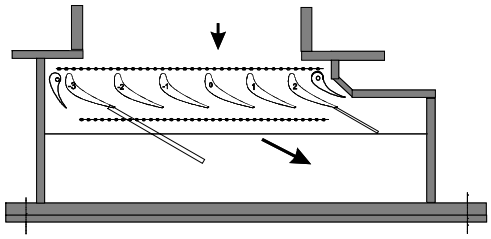

Fig. 10 *Setup with tailboards and without diffuser mounted*

The in Fig. 11 shown M_{iso} distribution at 98.9% and 109.4% of axial chord indicates an improved periodic flow field at the tip, this fact can be confirmed by looking also on the mean deviation shown in Table 3. The nearly matching M_{iso} close to the pressure side of NGV "1" and "0" confirms the fact, which can also be found in the published literature, that the pressure side is less sensitive to flow disturbances than the suction side.

	98.9%	***109.4%***
case 2		
ΔM	0.019	0.0277
s	0.011	0.0158
r	0.039	0.0584

Table 3 *ΔM, s, r in case 2 at 98.9% and 109.4% of c_{ax}*

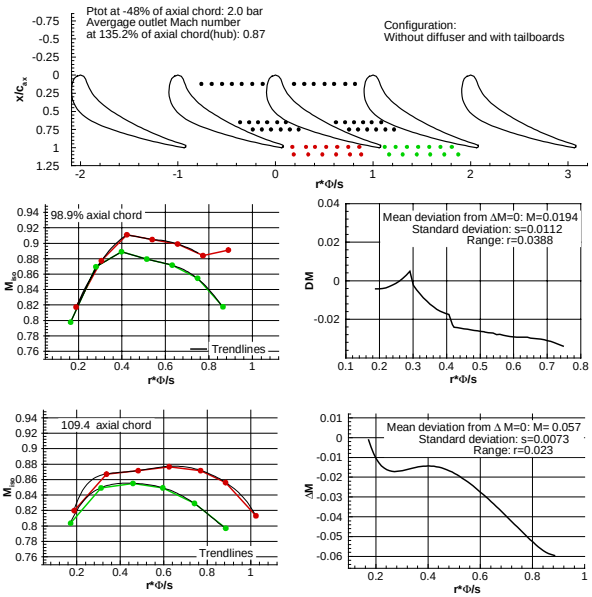

Fig. 11 *Tip M_{iso} distribution at 98.9% and 109.4% of axial chord (case 2)*

The hub M_{iso} distribution at 135.2% (Fig. 12) of axial chord also indicates a slightly better periodic outlet flow in flow passage "-1" and "-2". By dismounting the diffuser no improvements of the flow conditions in flow passage "+1" at the hub could be measured. The improved flow conditions measured in flow passage "+1" and "-1" at the tip leads to the conclusion of an influence of the tailboard mounted on NGV "2" on the outlet flow condition downstream of flow passage "+1" at the hub.

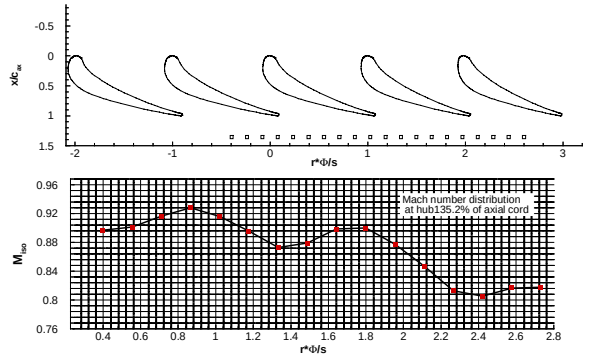

Fig. 12 *Hub M_{iso} distribution at 135.2% of axial chord (case 2)*

<u>Setup with one tailboard mounted on NGV -3 and with diffuser (case 3)</u>

The results achieved during the investigations in case 2 have not given a satisfied improved periodic outlet flow, this fact has led to the conclusion that only a change of the outlet diffuser alone has not a major impact on the flow conditions. Due to this the tailboard mounted on NGV +2 has been removed and the diffuser has been mounted again (Fig. 13).

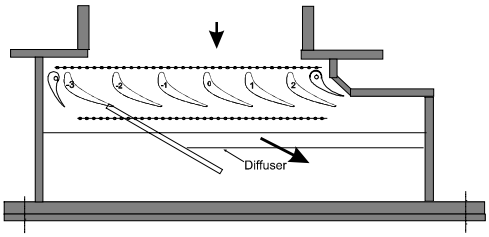

Fig. 13 *Setup with one tailboard mounted on NGV -3 and without diffuser*

The remounted diffuser has a significant impact on the quality of the outlet flow conditions, compared with case 2. The periodicity decreased 98.9% and 109.4% of axial chord at the tip. This fact is shown in Fig. 14. In Table 4 the mean deviation ΔM, standard deviation s and the range r for this two axial locations are given.

	98.9%	***109.4%***
case 3		
ΔM	0.046	0.046
s	0.011	0.004
r	0.032	0.021

Table 4 *ΔM, s, r in case 3 at 98.9% and 109.4% of c_{ax}*

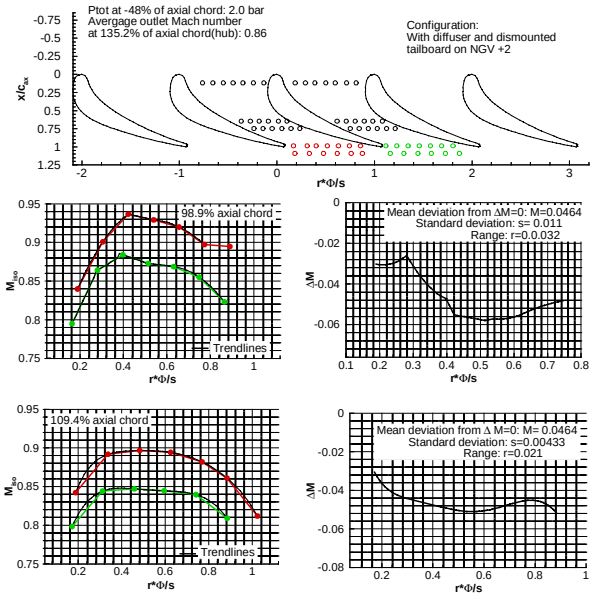

Fig. 14 *Tip M_{iso} distribution at 98.9% and 109.4% of axial chord (case 3)*

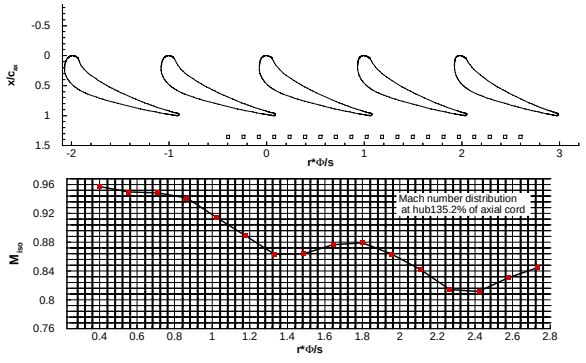

Fig. 15 *Hub M_{iso} number distribution at 135.2% of axial chord (case 3)*

The setup with the remounted diffuser and no tailboard mounted on NGV "+2" was a step backwards, the quality of the periodicity compared with case 1 and case 2 also decreased at the hub 135.2% of axial chord (Fig. 15).

Setup with one tailboard mounted on NGV -3 and without diffuser (case 4)

The results obtained in case 3 show a negative influence of the conical diffuser on the quality of the outlet flow conditions if the tailboard on NGV "+2" is dismounted. Further improvements of the periodicity were tried to achieve by changing the diffuser again into a step diffuser, the rest of case 4 has been kept the same as in case 3 (Fig. 16).

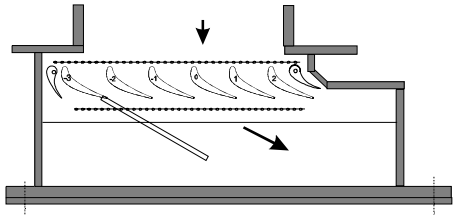

Fig. 16 *Setup with one tailboard mounted on NGV -3 and without diffuser*

Further improvements of the periodicity at the tip 98.9% and 109.4% of axial chord could be gained if the tailboard on NGV "+2" and the diffuser are dismounted (Fig. 17). The mean deviation ΔM, standard deviation s and the range r for this two axial locations are given Table 5.

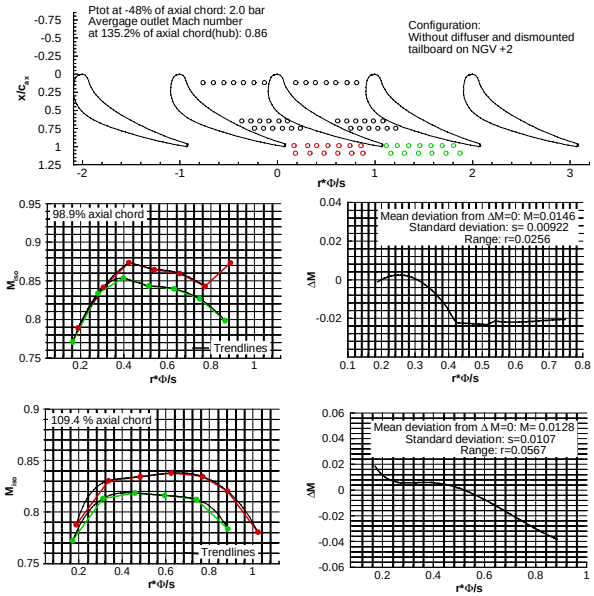

Fig. 17 *Tip M_{iso} distribution at 98.9% and 109.4% of axial chord (case 4)*

	98.9%	***109.4%***
case 4		
ΔM	0.015	0.013
s	0.007	0.011
r	0.023	0.057

Table 5 *ΔM, s, r in case 1 at 98.9% and 109.4% of c_{ax}*

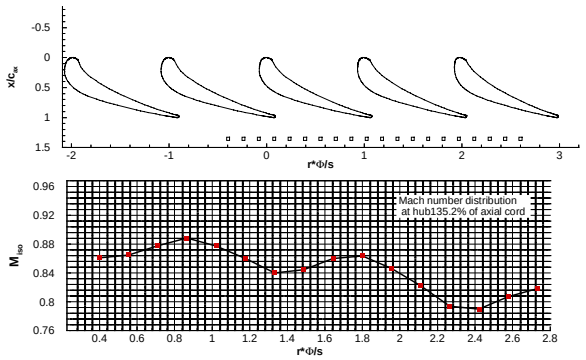

Fig. 18 *Hub M_{iso} distribution at 135.2% of axial chord (case 4)*

Fig. 18 shows an improved outlet periodicity also at the hub. This fact leads to the conclusion that the tailboard which was mounted on NGV "+2" and the conical diffuser, has introduced pressure disturbances downstream of the cascade which had an significant influence on the M_{iso} distribution in flow passage "+1". The dismounted tailboard and diffuser gave the outlet flow close to flow passage +1 and +2 the possibility to adjust itself. The outlet flow conditions with this configuration improved, but the result was still not acceptable for aerodynamic investigations. Due to this fact further modifications were necessary.

Setup without tailboards and without diffuser (case 5)

On the basis of the information achieved in case 4, in case five (Fig. 19) both tailboards and the diffuser were dismounted. This modification was done to give the outlet flow the possibility to adjust itself across the outlet section.

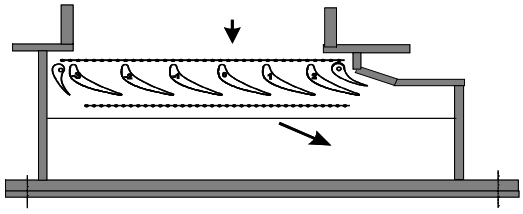

Fig. 19 *Setup without tailboards and without diffuser*

The outlet M_{iso} distribution at tip is illustrated in Fig. 20, because of the self adjusted outlet flow a nearly periodic flow could be achieved. This fact can be confirmed with the in Table 6 parameters given.

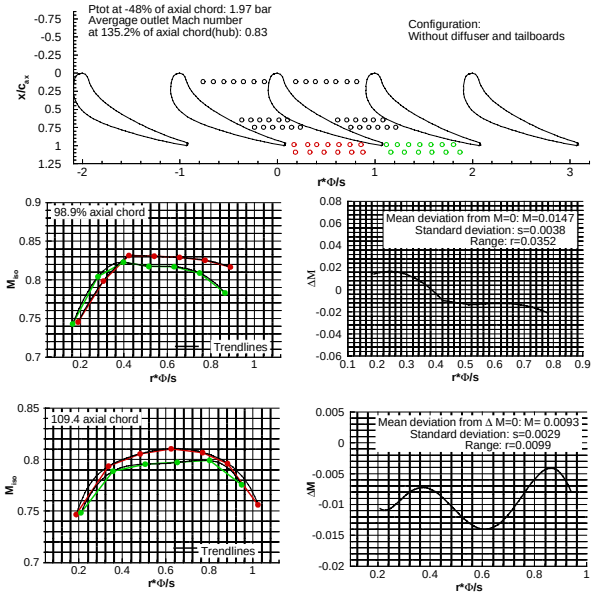

Fig. 20 *Tip M_{iso} distribution at 98.9% and 109.4% of axial chord (case 5)*

	98.9%	***109.4%***
case 3		
ΔM	0.015	0.009
s	0.004	0.003
r	0.035	0.01

Table 6 *ΔM, s, r in case 1 at 98.9% and 109.4% of c_{ax}*

The in Fig. 21 shown M_{iso} distribution at the hub also indicates an improved periodicity compared to the four other test cases.

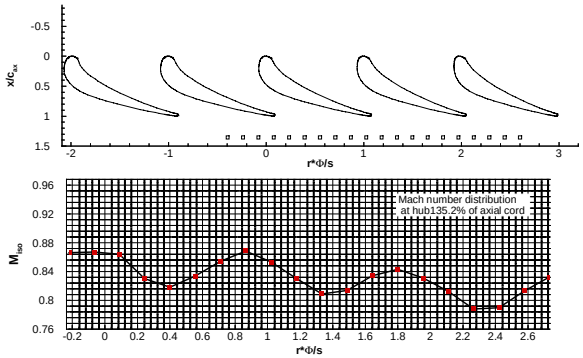

Fig. 21 *Hub M_{iso} distribution at 135.2% of axial chord (case 5)*

Conclusion

Due to this result it can be stated that the philosophy of tailboards is not applicable for this specific annular sector cascade facility with its geometrical restrictions and subsonic flow conditions. Nearly periodic flow conditions could be obtained when both tailboards were dismounted and a dump diffusion 190% downstream of axial cord has been used (case 5). Due to the use of a step diffusion and no tailboards the outlet flow angle adjusts itself to the downstream back pressure. Further test with the same arrangement have shown the repeatability of the results.

The inlet flow field was much less influenced by the modifications than the outlet flow.

The Final Setup

Case 5 has been selected for more detailed investigations of the inlet flow conditions. Fig. 22 shows the pressure distribution obtained by traversing a three hole probe, which has been aligned to the flow in the middle of the cross area. The pressure distribution shows a decreased measured pressure ratio p_{01}/p_{03} close to flow passage "-1" and "+1" and further to the left and right side wall. This result was obtained due to the angle sensitivity of the three hole probe, by locating the probe at position -1.3 and +1.3 and vanishing the left and right hole of the three hole probe for both position an inlet angle of +18° and -15° respectively, could be measured.

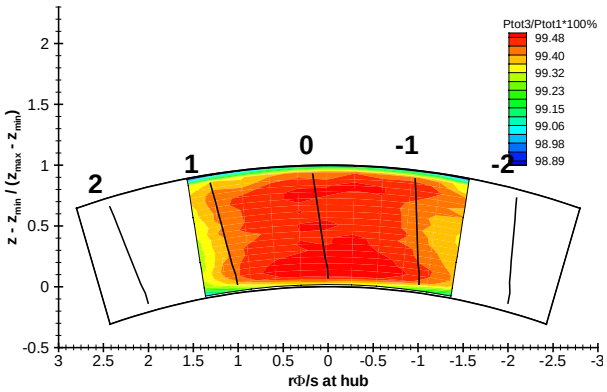

Fig. 22 *Inlet pressure distribution (case 5)*

The inlet M_{iso} distribution shown in Fig. 23. indicates a highly accelerated flow in flow passage +3 and -3 which is due to the size shape of the cross-sections close to these passages. The cross sections close to these two passages are much smaller than the flow passages between the vanes, this fact causes a suction of the flow field to the left and right.

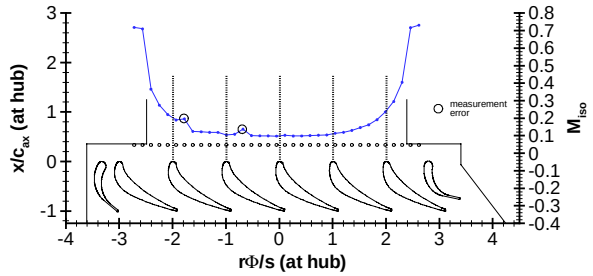

Fig. 23 *Inlet M_{iso} distribution (case 5)*

These results indicate that the flow upstream of the cascade is strongly non-uniform in the circumferential direction. The increase of the velocity towards the end walls at the inlet leads to the conclusion that both edge passages have a much higher through flow coefficient than the rest of the cascade. Due to the conservation of mass leads such an increase upstream of the cascade as well an

increase downstream of it. The effect can be modeled as follows.

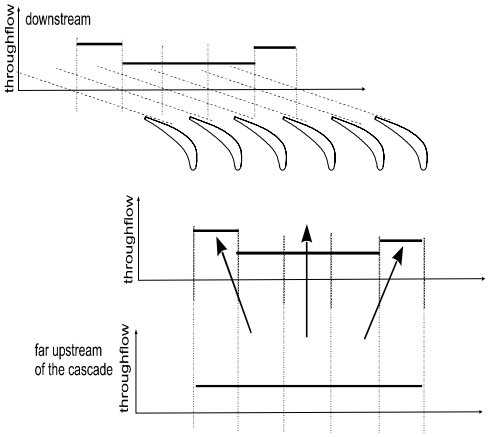

Fig. 24 *Edge passage with higher through flow coefficient and suction effect*

In Fig. 24, a schematic cascade with six blades is drawn. It is assumed that both edge passages have higher throughflow coefficients than the other passages in the cascade. Assuming a constant flow profile at a long distance upstream of the cascade, the flow will redistribute due to different throughflow coefficients of the cascade what can be described as suction effect of the edge passage. There is not only redistribution in mass flow but also a deviation of the originally parallel flow direction upstream the cascade to fulfill the conservation of momentum. This means that the incidence angle increases systematically from the middle flow passage to the walls, leading to an off-design incidence at the vane located away from the center.

The inlet flow field investigated has shown the necessity of further modifications of the test section to improve the inlet flow conditions in terms of achieving a homogenous inlet flow field. The final test section set up is shown in Fig. 25, the small cross areas which caused the suction in flow passage +3 and -3 have been tightened, the valve close to vane +2 closed.

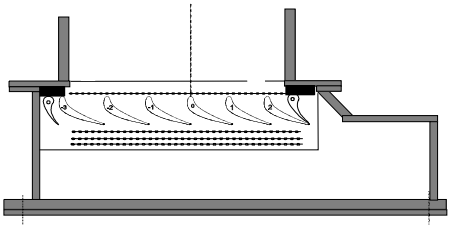

Fig. 25 *Final setup*

The inlet pressure distribution measured in the modified test section shows now a homogenous distribution (Fig. 26). The pressure losses caused by the honeycombs, mesh screens and the change of the geometry from round to a sector are 0.25%.

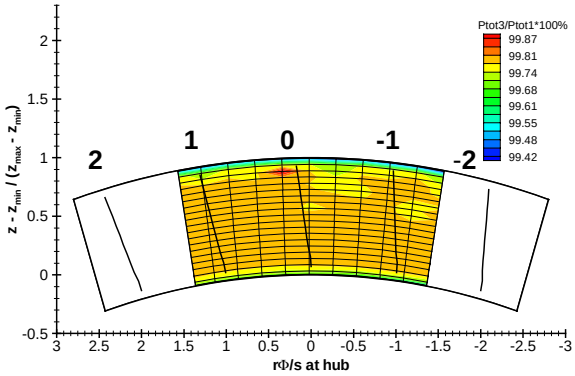

Fig. 26 *Inlet pressure distribution (seen from upstream, case 6)*

This result could be confirmed by measuring the inlet M_{iso} distribution shown in Fig. 27. Due to the location of the pressure taps -33% of c_{ax} upstream of the cascade the potential effect caused by the leading edge of the vanes can be observed.

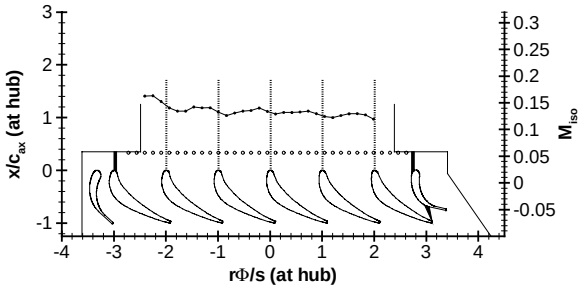

Fig. 27 *Inlet M_{iso} distribution (case 6)*

The in Fig. 28 contour plot of the isentropic Mach number distribution across flow passage “-1” and “+1” shows a fairly periodic flow field.

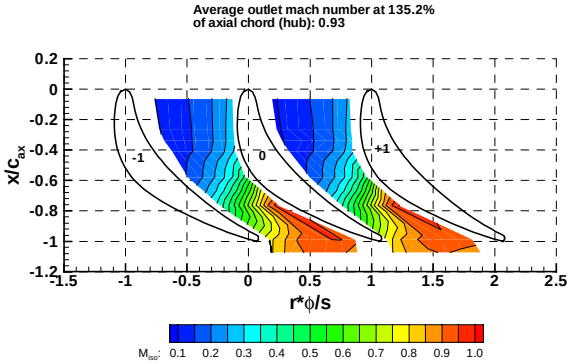

Fig. 28 *Contour plot of the M_{iso} distribution in flow passage -1 and +1 (case 6)*

<u>Profile M_{iso} distribution</u>

The local Mach number distribution along the vane profile is based on the ratio of the pressure measured at the vane surface through the pressure tap and the inlet total pressure upstream of the cascade. The profile M_{iso} distribution at $M_{2,is}$ = 0.8 and 0.9 measured at 50% span is shown in Fig. 28.

The M_{iso} at 41.3% of c_{ax} at the pressure side of NGV-1 and 49% of c_{ax} at the suction side confirms the periodicity of the flow for both flow conditions.

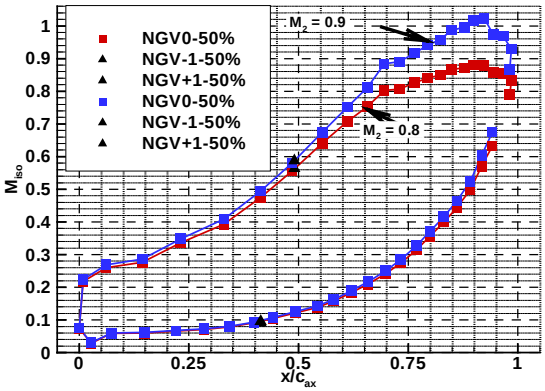

Fig. 29 *Profile M_{iso} distribution at 50% span*

Fig. 30 shows the suction side M_{iso} distribution 75% of span on NGV -1 and Fig. 31 the pressure side M_{iso} distribution at 25% span on NGV+1.

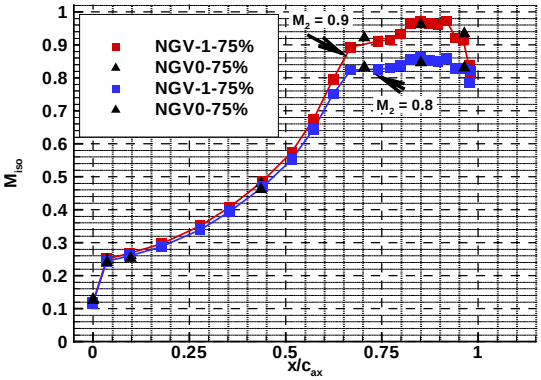

Fig. 30 *Profile M_{iso} distribution at 75% span on the suction surface*

The comparison of the profile M_{iso} distribution of NGV 0 at 25% span and 75% span with the profile M_{iso} distribution at 25% span on NGV+1 and M_{iso} distribution 75% of span on NGV -1 shows identical distributions on all three NGV's investigated. Due to this fact it can be concluded, that it is possible to achieve periodic flow conditions in an annular sector cascade facility.

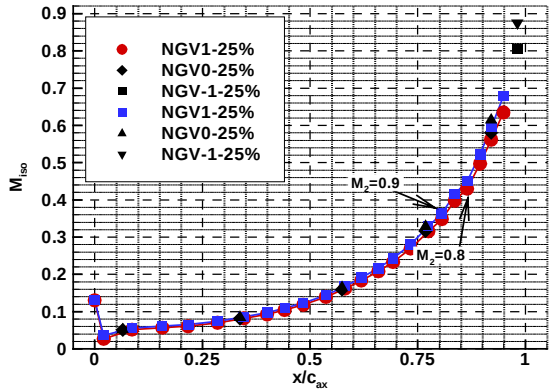

Fig. 31 *Profile M_{iso} distribution at 25% span on the pressure surface*

CONCLUSION

An annular sector cascade facility has been put into operation. A detailed description concerning the design and instrumentation has been given.

Five different validation test cases have been extensively investigated in order to obtain periodic flow conditions over at least two flow passages, passage "+1" and "-1". The investigations were focused on measuring the M_{iso} distribution across this two flow passages at the tip as well as 135.2% downstream of the cascade at hub.

Fairly good periodicity at the tip and hub could be obtained in case 5 where both the tailboards as well as the diffuser were dismounted. This fact leads to the conclusion that the use of a dump diffuser downstream of the cascade instead of a smooth guiding of the flow has a positive effect on the periodicity of the flow field. In the case where a dump diffuser is used the exit flow develops as a free jet and the flow angle adjusts itself to the downstream back pressure. It can also be stated, due to the findings, that the use of tailboards are not sufficient in subsonic flow conditions in an annular sector cascade.

Investigations of the M_{iso} distribution 33% of axial chord upstream at the hub as well as the traversing of a three hole probe 54% of axial chord in validation case five have shown inhomogeneous inlet flow conditions. This inhomogeneity was caused due to a suction effect in flow passage "+3" and "-3", which has been confirmed by surface flow visualizations at the inlet. By closing flow passage "+3" and "-3" homogeneous inlet flow conditions could be obtained, therefore also the periodicity of the flow at the outlet was increased.

Comparisons of the profile M_{iso} distribution measured on NGV "0" showed a fairly good agreement with the distribution measured on NGV "+1" and "-1". Due to this finding it can be concluded that one of the most important fact to achieve periodic flow conditions is the presence of identical stagnation streamlines at the outer blades in the cascade. The shape of these stagnation streamlines, however are very strongly affected by the flow in the outer by-pass channels.

ACKNOWLEDGEMENT

This work was initiated and supported, as part of the project Turbine Cooling Performance, supported within the Swedish Gas Turbine Center and funded by ABB-STAL, Volvo Aero Corporation and Energimyndigheten with Lic. of Engg. Sven Gunnar Sundkvist as the technical monitor. Thanks to Karl-Erik Andersson for the design of the annular sector test facility.

REFERENCES

Hoffs, A., Drost, U., Bölcs, A.; 1996
"Heat transfer measurements on a turbine airfoil at various Reynolds numbers and turbulence intensities including effects of surface roughness.", ASME Paper 96-GT-169

Curties, E.M, Hodson, H.P., Banieghbal M.R., Denton, J.D., Howell, R.J.; 1996
"Development Of Blade Profiles For Low Pressure Turbine Application", ASME Paper 96-GT-358

Kobayashi, H.; 1988
"Effect of Shock Wave Movement on Aerodynamic Instability of Annular Cascade Oscillating in Transonic Flow.", *ASME Paper 88-GT-187*

Lander, R.D., Fish, R. W., Suo, M. 1972
"External Heat Transfer Distribution on Film Cooled Turbine Vanes", J. of Aircraft, Vol.9, No 10, October 1972, pp. 707-714

Rådeklint, U. R., Hjalmarsson, C. S., Rubensdörffer, F. G., Jensen, J. F.; 1998
"A New Test Facility operating at Near-Engine Conditions for Testing of Cooled GT Components"**,** *ASME Paper 98-GT-557*

Rådeklint, U. R., Hjalmarsson, C. S., Rubensdörffer, F. G., Annerfeld, M.; 1999
"Experimental investigation of the external heat transfer on a nozzle guide vane"**,** *ImechE Conference Paper C557/119/99*

Wegener, D., Quest, J., Hoffman, W.; 1989
"Secondary Flow in a Turbine Guide Vane with Low Aspect Ratio.", *AGARD Conference Proceedings 468/469*

Wiers, S.-H.; Fransson, T. H.; 1998
"A new annular sector cascade test facility to investigate steady state cooling ef-fects *".*
14th Symposium on Measuring Techniques for Transonic and Supersonic Flow in Cascades and Turbomachines, University of Limerick, Wednesday 2st-Friday 4th September 1998

Wiers, S.-H.; 1999
"Design and Validation of an Annular Sector Cascade Facility", *Teknologie Licentiat Thesis, ISBN 91_7170-498_1*

Wiers, S.-H.; 2000
"Calibration of five hole pressure probes at the DLR Göttingen", *Internal Report, HPT/KTH 00-10*

Yamamoto, A.; 1987
"Production and Development of Secondary Flows and Losses in Two Types of Straight Turbine Cascade: Part1-A stator Case.", *Journal of Turbomachinery, Vol. 109, pp.186-193*